Electronic Supplementary Material (ESI) for Physical Chemistry Chemical Physics.

Supporting Information

Increase in the reduction potential of U(VI) upon interaction with graphene oxide surfaces

V. N. Bliznyuk[1*], N. Conroy[1], Y. Xie[1], R. Podila[2], A. Rao[2], B. A. Powell[1*]

[1] Department of Environmental Engineering and Earth Sciences, Clemson University, Clemson, SC 29634 USA

[2] Department of Physics and Astronomy, Clemson University, Clemson, SC 29634 USA

Index

Characterization and comparison of GO1 and GO2

GO1 and GO2 were characterized using powdered x-ray diffraction (XRD), X-ray photoelectron spectroscopy (XPS), and CHNS elemental analyzer for comparison. The XRD pattern was measured using a Miniflex x-ray diffractometer (Rigaku, Japan). A single peak was observed at ~10 degree (Figure S1) for GO1 while no peak was observed for GO2. GO itself has no lattice structure, the broad peak observed for GO1 is likely to be caused by the multilayer structure of GO1; while the absence of XRD pattern for GO2 indicating its monolayer structure. XPS measurements were performed using a Kratos AXIS Ultra DLD XPS system equipped with a hemispherical energy analyzer and a monochromatic Al K_α source. The monochromatic Al K_α source was operated at 15 keV and 150 W; pass energy was fixed at 40 eV for the detailed scans. All samples were prepared as pressed powders supported on a gold-plated stainless steel stub for the XPS measurements. C 1s and S 2p XPS spectra for GO1 and GO2 were obtained (Figure S2). All the spectra were calibrated using the 284.6 eV C-C peak. It can be seen from Figure S2 that the XPS spectra for GO1 and GO2 is similar, which indicated that they are similar material. The C 1s, and S 2p XPS spectra were further deconvoluted based on Gaussian function (processed in Igro Pro) (Figure S2). The ratio of the functional groups over total carbon/sulfur spectra for C 1s and S 2p spectra are calculated and listed in Table S1. For both GO1 and GO2, C 1s XPS spectra were deconvoluted based on previous studies [1-3] to peaks at ~284.5 eV, ~285.7 eV, ~286.6 eV, 287.54 eV, 288.94 eV, and ~292 eV corresponding to the planar C-C bonding, C-O bonding possibly from the attached hydroxyl functional group, C-O-C bonding from the epoxide group, >C-O from carbonyl functional group, carboxylic functional group, and π-π^* transition from graphite substrate. The ratio of functional group in Table S1 showing that: 1) Both GO1 and GO2 is consisted of approximately 50% carbon substrate; 2) The percentage of total oxygenated

functional groups for GO1 and GO2 is also comparable. 3) The XPS spectra indicated that GO1 containing higher amount of epoxide functional group while GO2 containing higher amount of phenolic group. 4) The amount of carbonyl plus carboxylate functional groups in GO1 and GO2 is comparable. The S 2p spectra for GO1 and GO2 were deconvoluted to peaks at 168 eV and 169 eV corresponding to sulfonate and sulfate respectively. The sulfonate to sulfur ratio for GO1 and GO2 is similar indicated the presence of both sulfonate and sulfate in both GO1 and GO2 due to the sulfuric acid fume procedure in Hummer's method. The CHNS elemental analysis was conducted with FlashEA 1112 elemental analyzer. BBOT ($C_{26}H_{26}N_2O_2S$) was used as a standard for carbon, hydrogen and sulfur quantification. The total carbon, hydrogen and sulfur content in GO1 and GO2 were listed in Table S2. The data in Table S2 shows that both GO1 and GO2 contains around 45% of total carbon; while GO2 contains a lot higher amount of sulfur than GO1, but possibly due to insufficient washing process during the manufacture of GO2.

The specific surface area (SSA) of GO1 and GO2 were obtained through N_2 (g) sorption BET analysis of the dry GO samples performed with a physisorption analyzer (Micromeritics ASAP 2020). For BET specific surface area measurement of GO1, 6 mL of GO1 stock solution was transferred to a biker and evaporated with moderate heat (<80 ºC); the dried GO1 samples were then vacuumed at < 100 ºC in a vacuum oven overnight to remove moisture and impurities in the sample. For GO2, it had to be pumped at < 100 ºC in a vacuum overnight to remove the moisture and impurities in the sample. The SSA of GO1 is measured to be 307 m^2/g and the SSA of GO2 is 50 m^2/g.

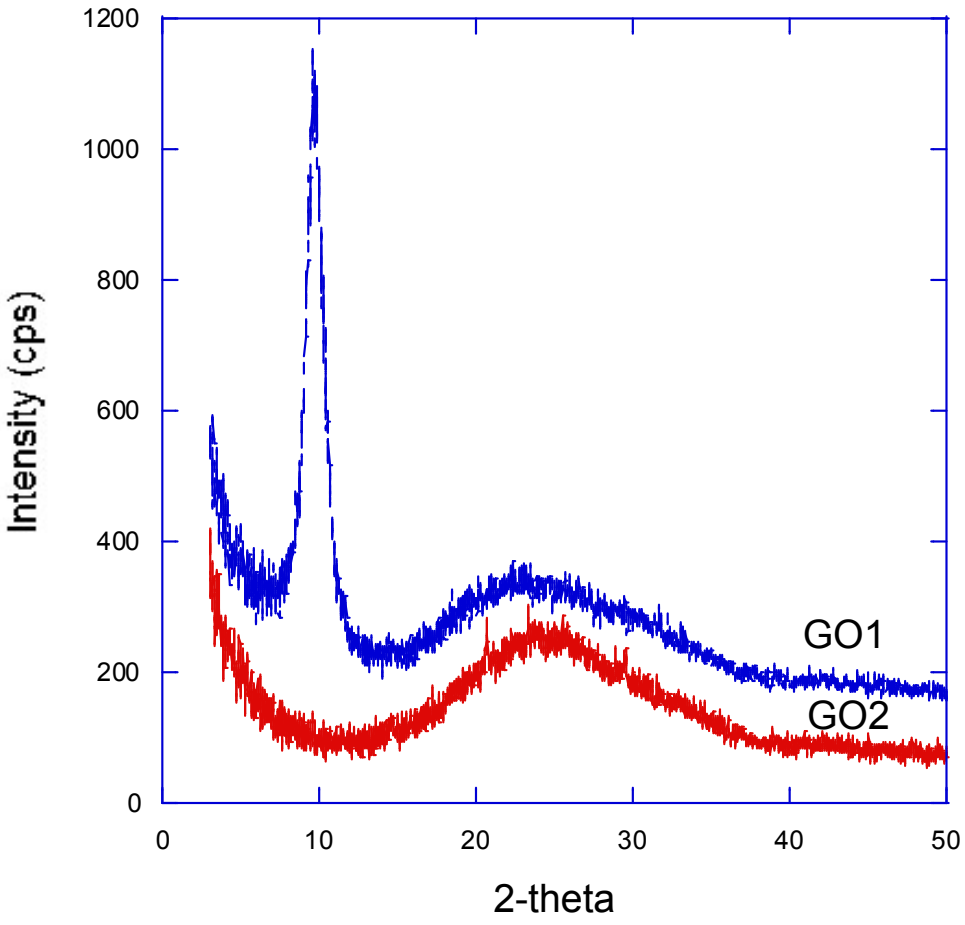

Figure S1. XRD plots for GO1 and GO2 samples. Samples for XRD experiments were cast on a solid substrate (glass) and dried overnight in air before the experiments. The broad peach from ~20-30 2-theta is from the glass slide.

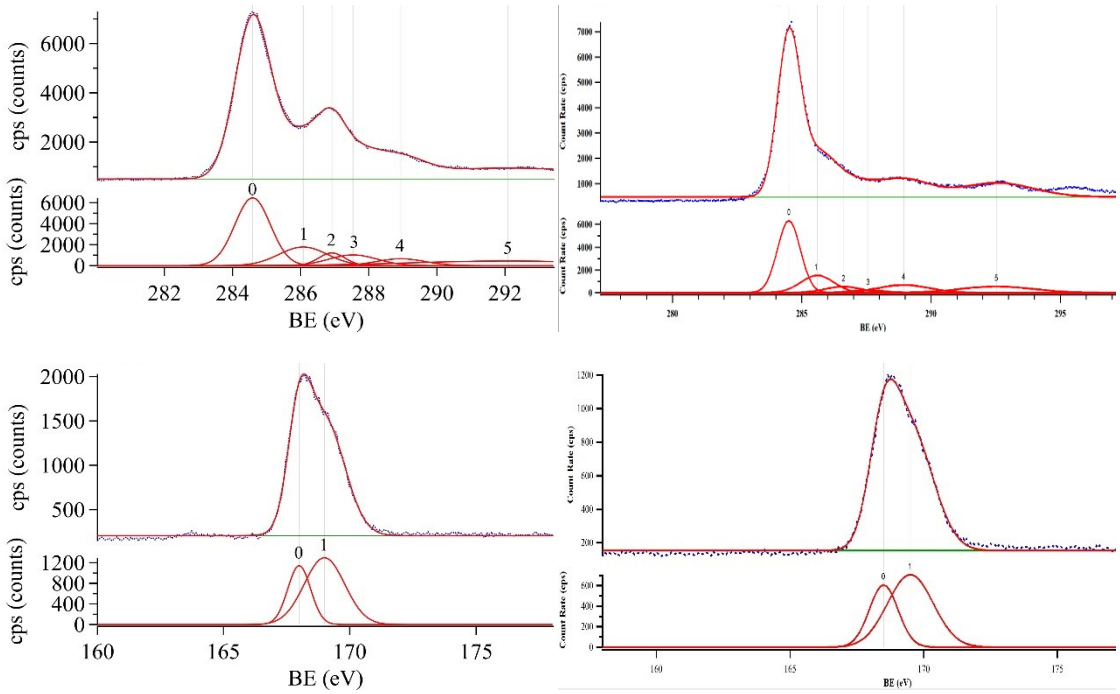

Figure S2. Comparison of the XPS C1s peaks for GO1 and GO2 (upper left and right), S2p peaks for GO1 and GO2 (lower left and lower right).

Table S1. Deconvoluted XPS peaks and area ratio for GO1 and GO2.

		GO1			GO2		
	Peak	BE (eV)	Area	Ratio	BE (eV)	Area	Ratio
C 1s	C-C	284.60	8673	0.47	284.5	6989	0.49
	C-O	285.70	1329	0.07	285.6	2427	0.17
	C-O-C	286.73	2906	0.16	286.6	951	0.07
	>C-O	287.54	1722	0.09	287.54	368	0.03
	COOH	288.94	1395	0.08	288.94	1698	0.12
	pi	292.08	2378	0.13	292.54	1963	0.14
S 2p	Sulfonate	168	1294	0.33	168.5	811	0.35
	Sulfate	169	2609	0.67	169.5	1517	0.65

Table S2. Comparison of the CHNS-O element analysis for GO1 and GO2

	GO1	GO2
Carbon	46 ± 0.90	42 ± 4.1
Hydrogen	2.0 ± 0.15	4.1 ± 0.3
Sulfur	3.9 ± 0.49	13 ± 0.2
Oxygen	35.5 ± 0.5	35.2 ± 0.5

Table S3. Comparison of physical properties of GO samples

	GO1	**GO2**
XRD (2 theta in degree)	10 degree	None
XPS	Similar shape and deconvolution	
Bulk C, H, S	Similar carbon and hydrogen content, higher sulfur in GO2	
SSA (m^2/g)	307	50

Degree of oxidation of GO materials

Table 2S summarizes elemental analysis data and gives approximately 35% oxidation value. Oxygen content in GOs under study can be estimated from XPS data (the ratio of C1s integral intensity for oxygen containing groups to the total intensity of C1s peak). In accordance to this calculation, the degree of oxidation is around 35% for both graphene oxides. This correspond to the reported value for commercially available GOs. High degree of oxidation for GO samples under study is also supported by Raman spectroscopy data (Figure S3). The degree of oxidation is proportional to the ratio of intensities of graphitic G band at ~1600 cm^{-1} and so-called defect (diamond) D-band at 1357 cm^{-1}. The ratio can be estimated as ~1.1, which corresponds to 35% oxidation of graphene in accordance to literature data [4,5].

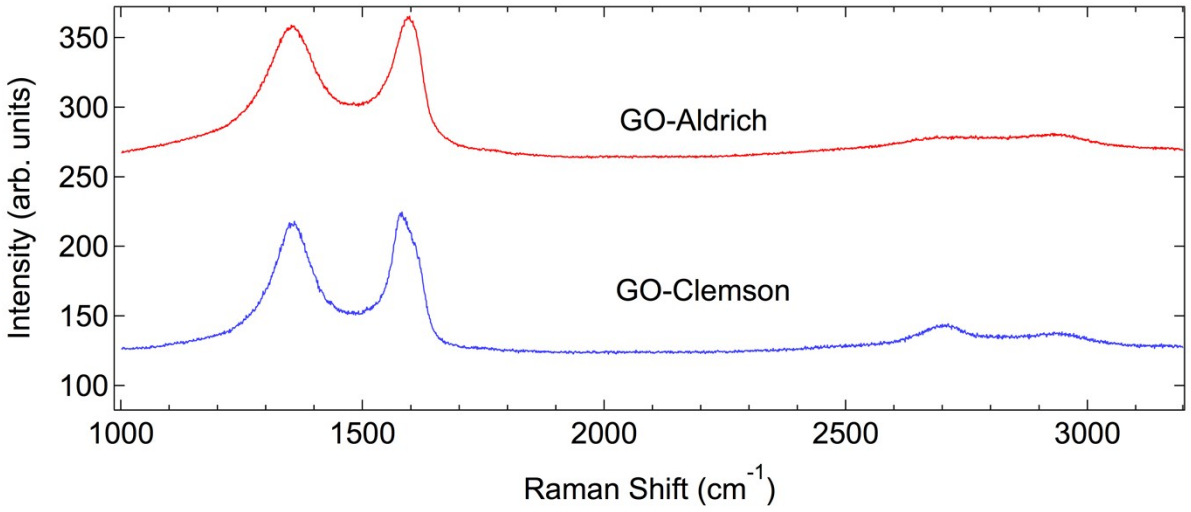

Figure S3. Raman spectra of GO1 (top) and GO2 (bottom) materials.

Reference CV curves (without uranium) for different working electrodes

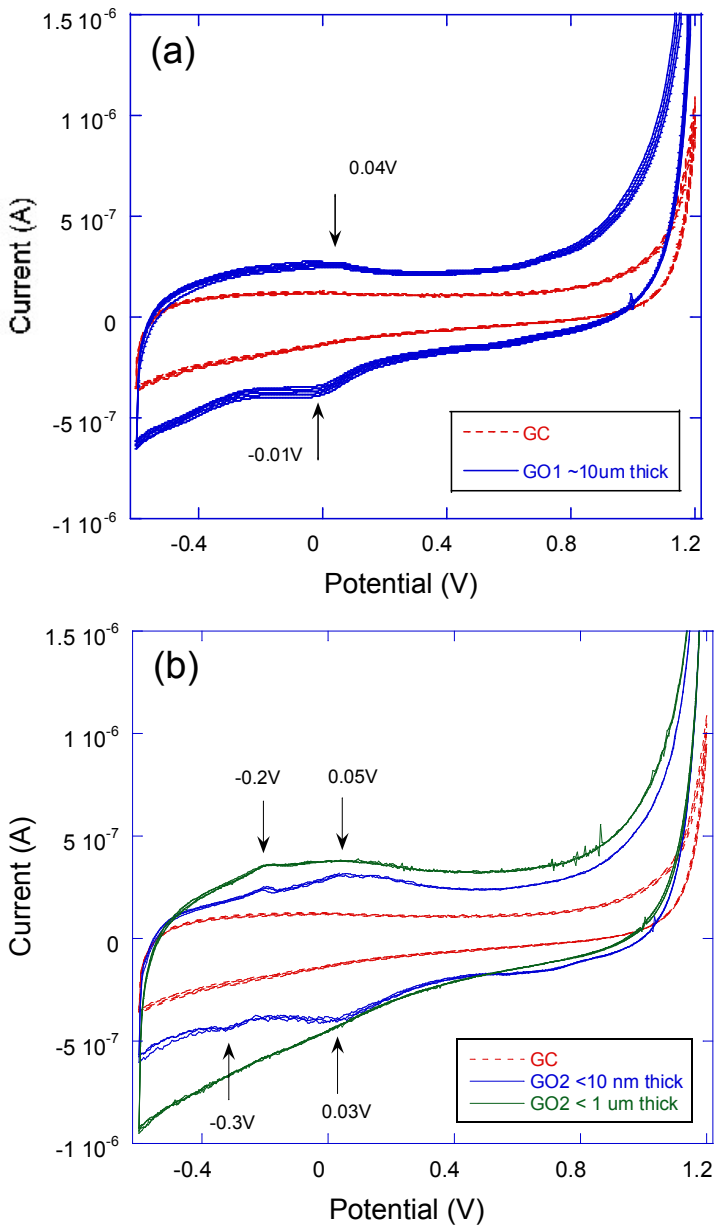

Figure S4. "Blank" CV voltammograms for GO1 (a) and GO2 (b) working electrodes recorded with 0.1 mM NaCl electrolyte. Voltammogram for a glassy carbon (GC) electrode shown for comparison. Scanning rate 10 mV/s in all cases. Note that current is at least one order of magnitude smaller than for uranyl electrolytes under study.

The Procedure of Areal Capacitance Calculation

The areal capacitance, C, of single electrodes measured in 3-electrode cells were determined by integrating the area under the normalized cyclic voltammetry curves (i.e., the current was divided by the scan rate and the area of the electrode with radius ~ 1.5 mm) over a voltage range (scanned at 10 mV/s) with no redox peaks, which was found to be 0-0.6 V for 0.1 M NaCl electrolyte (see Figure S5 below). The normalized capacitances for GO1 and GO2 were found to be ~ 5.25 and 148.5 μF/cm^2.

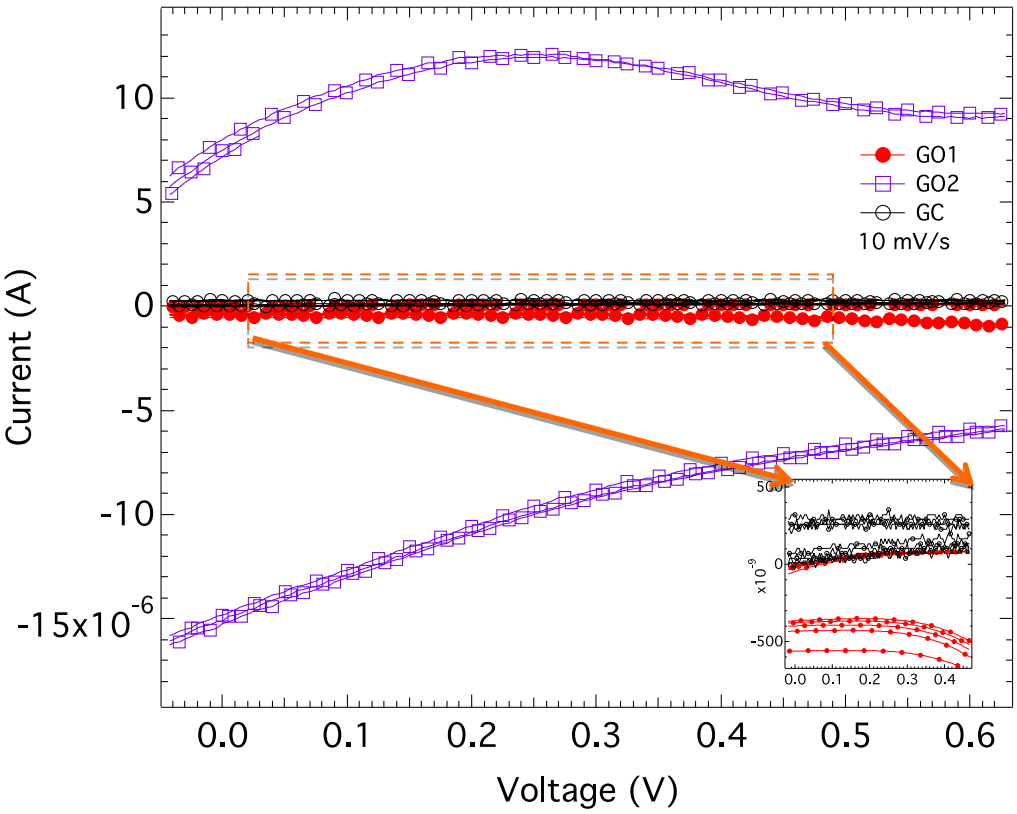

Figure S5: Cyclic voltammetry (CV curves) for GO1, GO2, and GC electrodes measured in 0.1 M NaCl at 10 mV/S scan rate. GO2 exhibited ~20-25 times higher current relative to GO1 and GC. A magnified view of the CV curves for GO1 and GC is shown in the inset.

The double layer capacitance for GO1 and GC electrodes was found to be very low ~ 5-6 μF/cm^2, as evidenced by the area of the CV curves (Figure S5). This suggests that the ions are unable to access pores situated deeper below the surface of GO1 leading to ion adsorption entirely on the surface. Given that GO1 and GC displayed similar areal capacitances, it is surmised that the electrolyte ions are unable to access high surface area and porosity of GO1 gleaned from BET N_2 gas adsorption measurements. Although the BET surface area of GO2 is appreciably lower than GO1, its porosity and single-to-few layer nature is more suitable for ion diffusion than multilayered GO2 leading to a significant increase in the areal capacitance. It is worth noting that redox peaks are not present in 0-0.6 V window for all the samples (GO1, GO2, and GC) and thus the possibility of pseudo-capacitance contributing to a high values in GO2 can be excluded. Based on the areal capacitance values derived from the CV curves, it is posited that the ion-accessible surface area of GO2 is at least >25-30 times higher than GO1 and GC.

The apparent disagreement between the BET surface area and areal capacitance was previously observed in different activated micro- and nanocarbon and polymers [6-9]. Qu et al. [9] rationalized this observation by distinguishing external and internal surface areas of nanomaterials, as described below. The surface area of a solid material is inversely related to the constituent particle size. In case of nanomaterials such as GO1 and GO2, the primary particles (e.g., a particle with layered sheets within GO1) often aggregate to stick together due to surface forces and thereby form secondary particles. Pores are formed in the secondary aggregated particles and thus the pore size depends on the size and shape of primary particles their packing configuration. While the external surface includes all the outer surface of secondary particles, and all of those cracks that are wider than they are deep, the internal surfaces comprise the walls of all cracks, pores and

cavities that are deeper than they are wide. The external pores are much easier to be accessed by electrolyte than those of internal pores. Thus, in case of GO2, the better accessibility of pores results in an increased capacitance.

References

[1] Ganguly, A.; Sharma, S.; Papakonstantinou, P.; Hamilton, J. Probing the thermal deoxygenation of graphene oxide using high- resolution in situ X-ray-based spectroscopies. *J. Phys. Chem. C* **2011**, 115 (34), 17009−17019.

[2] Stankovich, S.; Dikin, D. A.; Piner, R. D.; Kohlhaas, K. A.; Kleinhammes, A.; Jia, Y.; Wu, Y.; Nguyen, S. T.; Ruoff, R. S. Synthesis of graphene-based nanosheets via chemical reduction of exfoliated graphite oxide. *Carbon* **2007**, 45 (7), 1558−1565.

[3] Chandra, V.; Park, J.; Chun, Y.; Lee, J. W.; Hwang, I.-C.; Kim, K. S. Water-dispersible magnetite-reduced graphene oxide composites for arsenic removal. *ACS Nano* **2010**, 4 (7), 3979−3986.

[4] Gupta, N. Sharma, U. Singh, M. Arif, A. Singh, Higher oxidation level in graphene oxide, Optik, 143 (2017) 115–124

[5] J. Guerrero-Contreras, F. Caballero-Briones, Graphene oxide powders with different oxidation degree, prepared by synthesis variations of the Hummers method, Materials Chemistry and Physics, 153 (2015) 209-220

[6] Mosch, H. L. K. S., Akintola, O.; Plass, W.; Höppener S.; Schubert, U.S.; Ignaszak, A. Specific Surface versus Electrochemically Active Area of the Carbon/Polypyrrole Capacitor: Correlation of Ion Dynamics Studied by an Electrochemical Quartz Crystal Microbalance with BET Surface. *Langmuir* **2016**, *32* (18), 4440–4449.

[7] Liu, H.; Zhang, Y.; Ke, Q.; Ho, K.H.; Hu, Y.; Wang, J. Tuning the porous texture and specific surface area of nanoporous carbons for supercapacitor electrodes by adjusting the hydrothermal synthesis temperature. *J. Mater. Chem. A*. **2013**, 1, 12962-12970.

[8] Endo, M.; Kim, Y. J.; Takeda, T.; Maeda, T.; Hayashi, T.; Koshiba, K.; Hara, H.; Dresselhaus, M. S. Poly(vinylidene chloride)-Based Carbon as an Electrode Material for High Power Capacitors with an Aqueous Electrolyte. *J. Electrochem. Soc.* **2001**, 148 (10), A1135-A1140

[9] Qu, D.; Shi, H. Studies of activated carbons used in double-layer capacitors. *Journal of Power Sources* **1998**, 74, 99-107.